May 2000 • NREL/ SR-520-28376

Subcontractor Report

In-Situ Sensors for Process Control of $CuIn(Ga)Se_2$

Phase II Annual Report
February 1999—February 2000

I.L. Eisgruber, J.R. Engel, R. Treece,
and R. Hollingsworth
Materials Research Group, Inc.
Wheat Ridge, Colorado

National Renewable Energy Laboratory

1617 Cole Boulevard
Golden, Colorado 80401-3393

NREL is a U.S. Department of Energy Laboratory
Operated by Midwest Research Institute • Battelle • Bechtel

Contract No. DE-AC36-99-GO10337

May 2000 • NREL/ SR-520-28376

In-Situ Sensors for Process Control of $CuIn(Ga)Se_2$

Phase II Annual Report February 1999—February 2000

I.L. Eisgruber, J.R. Engel, R. Treece, and R. Hollingsworth
Materials Research Group, Inc.
Wheat Ridge, Colorado

NREL Technical Monitor: H.S. Ullal

Prepared under Subcontract No. ZAK-8-17619-08

National Renewable Energy Laboratory

1617 Cole Boulevard
Golden, Colorado 80401-3393

NREL is a U.S. Department of Energy Laboratory
Operated by Midwest Research Institute • Battelle • Bechtel

Contract No. DE-AC36-99-GO10337

NOTICE

Available electronically at http://www.doe.gov/bridge

Available for a processing fee to U.S. Department of Energy
and its contractors, in paper, from:

U.S. Department of Energy
Office of Scientific and Technical Information
P.O. Box 62
Oak Ridge, TN 37831-0062
phone: 865.576.8401
fax: 865.576.5728
email: reports@adonis.osti.gov

Available for sale to the public, in paper, from:

U.S. Department of Commerce
National Technical Information Service
5285 Port Royal Road
Springfield, VA 22161
phone: 800.553.6847
fax: 703.605.6900
email: orders@ntis.fedworld.gov
online ordering: http://www.ntis.gov/ordering.htm

Printed on paper containing at least 50% wastepaper, including 20% postconsumer waste

LIST OF FIGURES

LIST OF TABLES

TABLE OF CONTENTS

1. Introduction

The use of in-situ sensors for process control is an important aspect in improving the manufacturability of thin-film $CuIn_xGa_{1-x}Se_2$ (CIGS) modules, since yield and reproducibility issues remain a significant challenge in CIGS photovoltaic module fabrication. Materials Research Group (MRG), Inc. is developing in-situ sensors to improve yield, reproducibility, average efficiency, and prevention of "lost processes". In-situ x-ray fluorescence (XRF) is under development to monitor composition and thickness of deposited layers, and in-situ optical emission spectroscopy (OES) is under development for real-time feedback describing the deposition plasma. MRG is addressing these issues as a "Research and Development Partner". The largest portion of the work performed in Phase II concerns development of a method to accurately measure CIGS film thicknesses and compositions via XRF, in a manner consistent with in-situ, real-time monitoring of the deposition process. This work includes advances in the design of the x-ray sensor itself, the analysis of the x-ray signals, protection of the sensor in the Se environment, and deposition chamber installation issues. The following sections describe each of these areas of progress in more detail.

2. Low-Cost System Design and Assembly

An important area Phase II progress was the design and assembly of a low-cost XRF sensor at MRG. The sensor is built entirely of commercially-available and cost-effective components, and is fully controllable by custom software for CIGS deposition. A photograph of the sensor, installed on a standard vacuum tee, is shown in Figure 1. Measurements on the system demonstrated good agreement between measured and theoretical count rates in simple systems. For example, the data points in Figure 2 show the Cu-Kα emission as a function of thickness for thin Cu films. Error bars in the x-direction represent mechanical profilometer uncertainty. Error bars in the y-direction show the magnitude of fluctuation in the x-ray tube current. The line demonstrates the relationship expected from theory for the thicknesses shown. The agreement between theory and experiment can also be extended to very thick samples, within the uncertainty created by not precisely knowing the spectral distribution of the continuous radiation emitted from the x-ray tube.

Figure 1: XRF sensor designed and assembled at MRG.

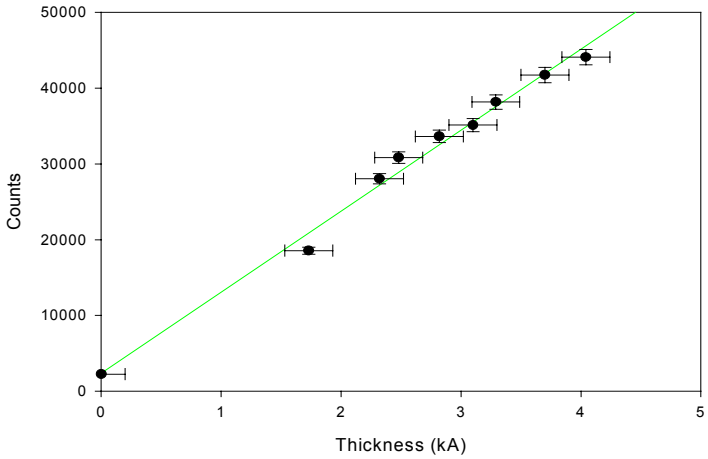

Figure 2: Counts from Cu emission as a function of Cu film thickness.

3. Data Analysis

A number of advances were made during Phase II in the interpretation of data from the low-cost XRF sensor described in the previous section. In this section, XRF measurements are compared with inductively coupled plasma (ICP) measurements. Results are compared in terms of atomic ratios and and effective element thicknesses. (XRF and ICP both measure atoms per sample area for each constituent element. For more intuitive interpretation, atoms per sample area is converted to effective element thickness by use of the elemental density and atomic weight.)

Compositions extracted from XRF measurements using the prototype sensor have shown good agreement with inductively ICP measurements, over a large variety of samples. An example of results of ex-situ XRF measurements are shown in Figure 3. The x-axis shows the ratio Cu/(In+Ga) as measured by ICP at the National Renewable Energy Laboratory (NREL) by Raghu Bhattacharya. The y-axis shows Cu/(In+Ga) as measured by x-ray fluorescence. Error bars in the x-direction represent uncertainty in the ICP measurement, whereas error bars in the y-direction reflect noise in the XRF measurement and error due to sample nonuniformity. The range of elemental compositions in the samples of Figure 3 span high-efficiency CIGS samples by an appreciable percent. High efficiency CIGS devices

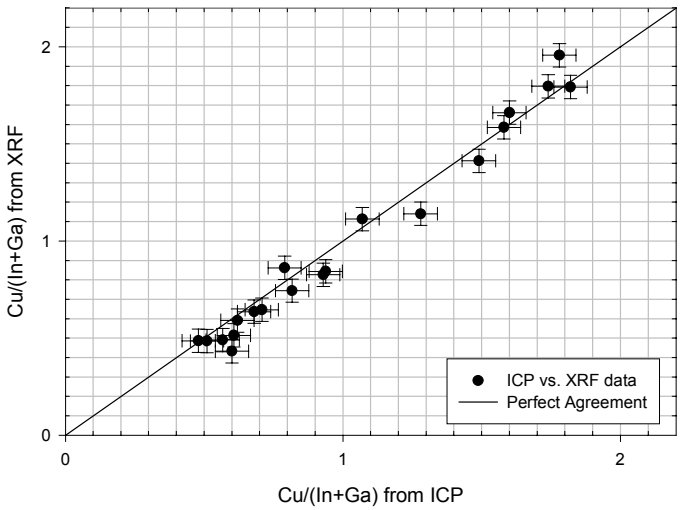

Figure 3: Comparison of the ratio Cu/(In+Ga) as measured by ICP and XRF.

typically contain about 3100 Å Cu, 5200 Å In, 1300 Å Ga, and 15000 Å Se. Cu thicknesses in the samples of Figure 3 range from 500 to 3600 Å, In thicknesses range from 600 to 16000 Å, Ga thicknesses range from 0 to 8400 Å, Se thicknesses range from 8100 to 31000 Å, and Mo thickness range from 0.25 to 1.1 μm. Substrates were soda-lime glass, lightweight aerospace glass, and polyimide. Measurement time was 60 seconds, and data processing time is about 5 seconds. Through adaptations in x-ray spot size and x-ray tube current, similar measurement times will be used when the components are installed in-situ. When only samples with similar thicknesses and substrates are compared, agreement between XRF and ICP composition measurements is even closer than that seen in Figure 3.

The real-time XRF analysis is based on a first-principles pre-calculation of coefficients needed to convert signal to composition. Figure 4 shows how multiple levels of sophistication in the XRF interpretation improve the agreement between XRF and ICP measurements. The triangles in figure Figure 4 show the results obtained for the simplest interpretation. In this case, a calibration sample is measured, and for all subsequent samples, the percent change in the in the amount of emission from any element is assumed to be the same as the percent change in the amount of that element present. Significant disagreement exists for samples with elemental thicknesses far from the calibration sample. The empty circles in Figure 4 show one further level of sophistication introduced into the calculation. In this case, nonlinearities in counts versus thickness are accounted for by first-principles calculations. The filled circles show the full calculation, as in the previous figure, and the best agreement. The full interpretation is completed by using a known back contact signal (or substrate signal, if steel substrates are used) to correct for fluctuations in x-ray tube intensity.

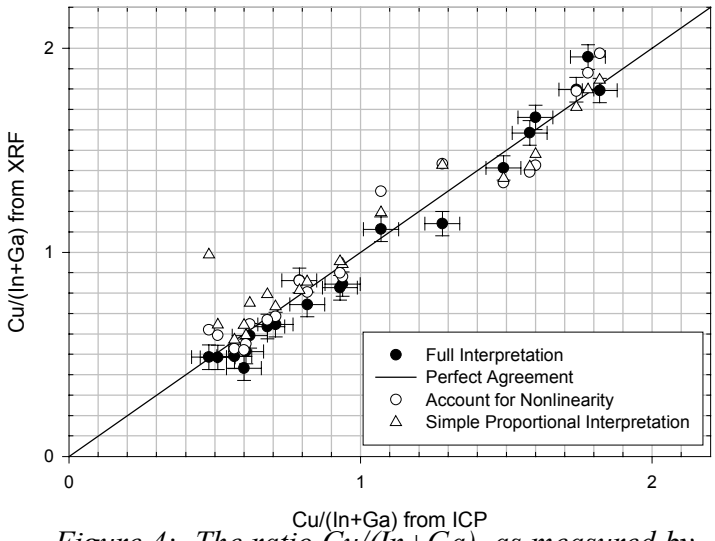

Figure 4: The ratio Cu/(In+Ga), as measured by XRF and ICP, showing multiple levels of sophistication in the XRF interpretation.

The use of a low-cost x-ray sources and detectors requires introduces some complexity into the XRF measurement. Interpretation must be successful despite lower detector resolution and lack of higher energy x-rays, when compared to more expensive equipment. Correct assessments of the amount of In and Ga present can be particular challenges, since the high energy In-Kα peak is barely excited, and the Ga-Kα peaks and Cu-Kβ peaks overlap in energy. Data intpretation from the low-cost sensor has, however, accurately indicated the amounts of In and Ga in samples. For example, Figure 5 shows

In thickness ratio on a series of samples as measured by XRF and ICP. The samples were made at Lockheed Martin Astronautics by changing the transport speed as a 12" x 12" CIGS piece passed through the Ga deposition zone, thus grading the Ga content across the device. Each sample was cut from a different position along the 12" parallel to the transport (graded) direction. In the direction perpendicular to the transport direction, one piece was cut for ICP measurement, and two pieces were cut for XRF measurements, one on either side of the ICP piece. In Figure 5, triangles show the ICP results, while circles and squares show the XRF results on the two series of XRF samples. The vertical line indicates the sample used for measurement calibration. The samples measured contain a variation in In thickness from 600 to 1800 Å. The amount of In in these samples is much less than the typical 5200 Å contained in a 2.5 µm CIGS film with a Ga/(In+Ga) ratio of 0.25. Nevertheless, the XRF and ICP measurements yield the same In thicknesses. Figure 6 illustrates the improved sensitivity of Ga measurements through analysis of an alternate Ga emission line. The ratio Cu/(In+Ga) is shown versus position on the same sample set as in Figure 5. Triangles show ICP measurements, filled circles show XRF measurements made with the initial choice of Ga emission, and hollow squares show the improved interpretation results.

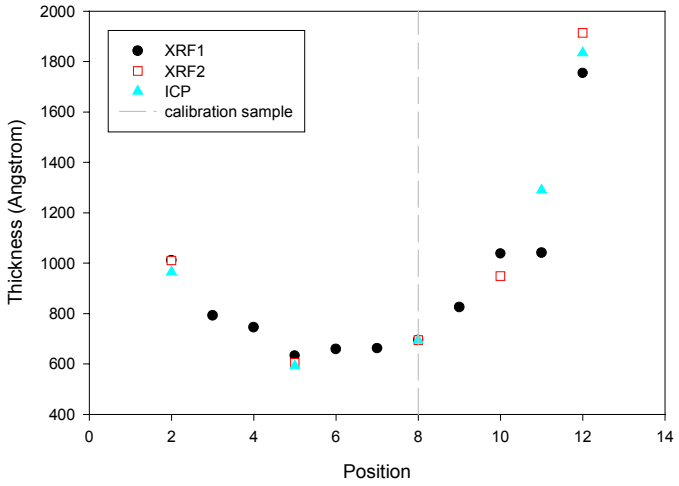

Figure 5: In thickness as a function of position on a large graded sample.

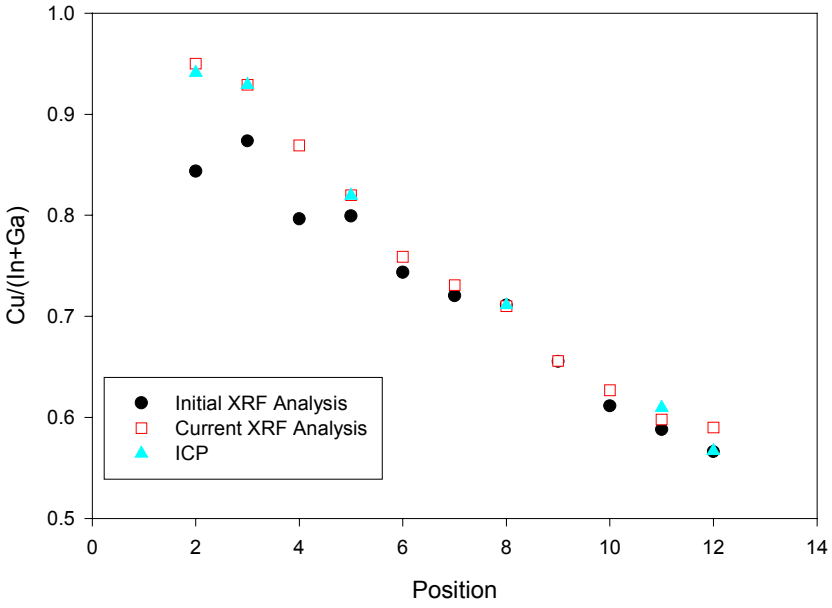

Figure 6: The ratio Cu/(In+Ga) as a function of position on a large graded sample.

4. Sensor Protection

A critical aspect of installing the XRF sensor in-situ is protecting the sensor from Se and from thermal loads. Hardware is currently under design that will allow the sensor to operate with ambient temperatures of 200 ^{o}C and Se pressure. Sensor parts will be cooled. They will be shielded from Se by a baffle that requires any Se atom travelling toward the sensor to undergo multiple collisions with a cooled surface. Supplied and detected x-rays will travel to the sensor through inexpensive polymer windows. The x-ray absorption of these windows has been measured at MRG and was found to be low enough for sensor operation. Figure 7 shows the fluorescence spectrum of a CIS sample with and without polymer windows installed. At all but the lowest energies, the absorption of the windows is negligible, and even at the lowest energies the transmitted signal is appreciable. The polymer windows will be heated to drive off Se, and can be easily replaced if necessary. Four important characteristics of the sensor protection hardware are to be tested immediately: sufficient cooling of the sensor in a 200 ^{o}C ambient, the lack of coating of the sensor with Se, reasonable polymer window lifetime, and successful removal of Se from the windows during deposition. Assembly for such tests is in progress.

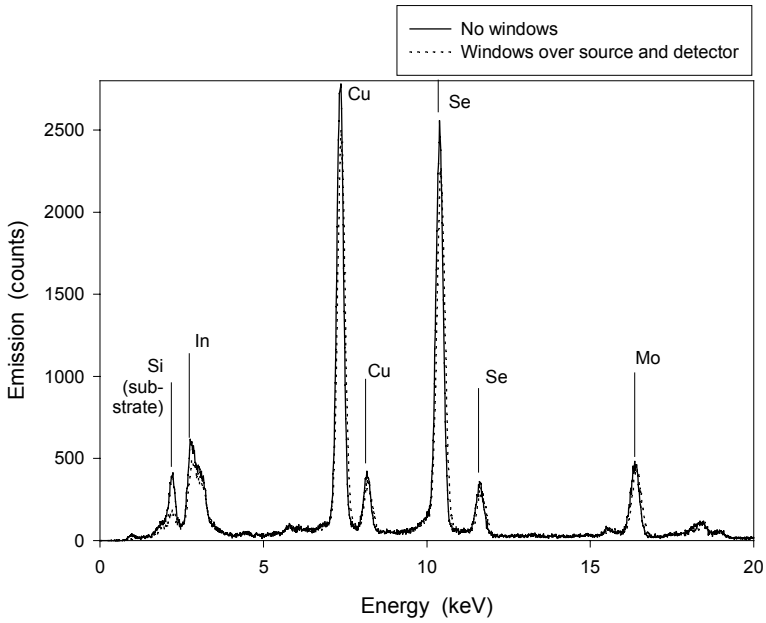

Figure 7: Fluorescence spectrum of CIS sample with and without polymer windows installed.

5. Installation issues

A number of installation issues must be considered when adaptating the prototype sensor, initially operated ex-situ, to an in-situ environment. An important concern is maintaining count rate when sensor to sample distance is increased. Table 1 shows the operating conditions for the prototype sensor during the acquisition of the data in the previous figures. Table 2 shows operating conditions for the sensor that would increase sample-to-sensor distance, produce the same count rates as those currently measured, and require only minor equipment modifications. The increase in sample-to-sensor distance is achieved by increasing the x-ray tube current and allowing a slightly larger spot size. Further increases in sample-to-sensor distance might be achieved by longer acquisition times, larger spot sizes, or tolerating increased uncertainty in composition. MRG is

Source to sample distance	**6.4 cm**
Sample to detector distance	**5 cm**
Acquisition time	**60 sec.**
X-ray beam spot size	**1.6 cm^2**
X-ray tube current	**100 µA**

Table 1: Current operating conditions for prototype sensor.

Source to sample distance	**14.4 cm**
Sample to detector distance	**14.4 cm**
Acquisition time	**60 sec.**
X-ray beam spot size	**3.2 cm^2**
X-ray tube current	**1 mA**

Table 2: Equivalent operating conditions for prototype sensor.

working with industrial partner Global Solar Energy (GSE) to install the XRF sensor on a CIGS production chamber. Minimum sensor to sample distance in the location identified at GSE is 8 cm.

A number of other aspects of installing the sensor in-situ have also been advanced this quarter. First, the minimum energy resolution of the detected x-rays for effective composition extraction was determined. The energy resolution is affected by the detector temperature and vibration. Resolution as a function of vibration was measured and compared with vibration measurements at prospective installation sites at GSE and MRG. Vibration at those locations was determined to be small enough for adequate sensor resolution. Second, initial composition measurements were made on CIGS on steel substrates. (Earlier measurements were made on CIGS on glass substrates.) It was found that composition of CIGS on steel substrates can be measured, as long as x-ray illumination is decreased slightly to avoid saturating the detector with counts from the substrate. Third, a number of operation characteristics of the sensor were specified. These characteristics include x-ray spot size, measurement time, sample-to-sensor distance, maximum operating temperature, sensor output, mounting requirements, water flow requirements, power requirements, alarms, safety interlocks, and calibration options.

Finally, the software for the automatic extraction of composition data and sensor operation is largely intact. An example screen is shown in Figure 8. The analytical foundation for the software has already been established and tested. However, the software needs to be expanded to quote uncertainties as a function of sample and measurement conditions, to remove all required operator intervention, to communicate pertinent data to the deposition chamber controls, and to allow easy calibration.

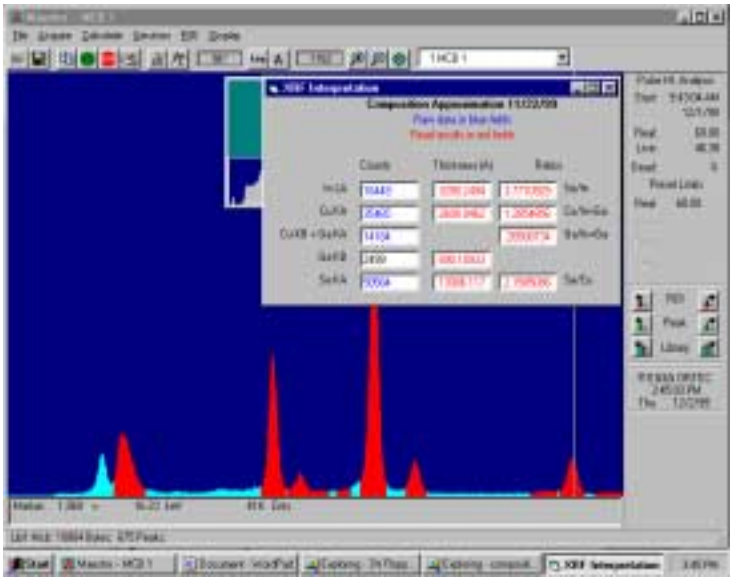

Figure 8: Software for extracting CIGS composition information from XRF sensor.

6. Conclusions

Progress toward the development in-situ sensors for CIGS during Phase II includes

- design and assembly of a low-cost XRF sensor suitable for in-situ use and real-time control;
- demonstration of agreement between theory and experiment for XRF measurement simple systems using the XRF sensor;
- demonstration of agreement between ICP and XRF results over a wide variety of CIGS samples;
- initial design of hardware protecting XRF sensor in heated, Se ambient;
- resolution of a number of installation issues, including specification of measurement time versus sensor-to-sample distance, utilities requirements, and vibration restrictions;
- development of software for sensor operation and the automatic extraction of composition data; and
- interaction with CIS National Team industrial partners to specify and adapt sensor functions.

7. Future Plans

A number of issues relating the real-time control of deposition using XRF are scheduled to be addressed immediately. First, the hardware protecting the sensor from Se and thermal loads is currently undergoing testing. When this hardware is operating satisfactorily, the plate used to install the XRF sensor and Se protection onto the deposition chamber will be built. Safety interlocks to protect the equipment and workers will be incorporated. The system will be installed and tested in-situ, including a test run at GSE. Software will be refined to allow easy calibration, require no operator intervention, quote uncertainties as a function of sample and measurement conditions, and communicate pertinent data to the deposition chamber controls.

Some investigations relating to window layers and OES are also planned for Phase III. XRF sensing of CdS, ZnO, and ITO will be evaluated. The relationships between deposition rates and plasma emissions of absorber and window materials will be obtained.

REPORT DOCUMENTATION PAGE

Form Approved
OMB NO. 0704-0188

1. AGENCY USE ONLY (Leave blank)	2. REPORT DATE	3. REPORT TYPE AND DATES COVERED
	May 2000	Phase II Annual Subcontract Report, 15 February 1999–14 February 2000

4. TITLE AND SUBTITLE
In-Situ Sensors for Process Control of CuIn(Ga)Se_2; Phase II Annual Subcontract Report, 15 February 1999–14 February 2000

5. FUNDING NUMBERS
C: ZAK-8-17619-08
TA: PV005001

6. AUTHOR(S)
I.L. Eisgruber, J.R. Engel, R. Treece, and R. Hollingsworth

7. PERFORMING ORGANIZATION NAME(S) AND ADDRESS(ES)
Materials Research Group, Inc.
12441 W. 49th Ave., Suite #2
Wheat Ridge, CO 80033-1927

8. PERFORMING ORGANIZATION REPORT NUMBER

9. SPONSORING/MONITORING AGENCY NAME(S) AND ADDRESS(ES)
National Renewable Energy Laboratory
1617 Cole Blvd.
Golden, CO 80401-3393

10. SPONSORING/MONITORING AGENCY REPORT NUMBER
SR-520-28376

11. SUPPLEMENTARY NOTES
NREL Technical Monitor: H.S. Ullal

12a. DISTRIBUTION/AVAILABILITY STATEMENT
National Technical Information Service
U.S. Department of Commerce
5285 Port Royal Road
Springfield, VA 22161

12b. DISTRIBUTION CODE

13. ABSTRACT *(Maximum 200 words)*
This report summarizes the work performed by Materials Research Group, Inc., in Phase II of this subcontract. Progress toward the development of in-situ sensors for CuIn(Ga)Se_2 (CIGS) during Phase II includes:

- design and assembly of a low-cost X-ray fluorescence (XRF) sensor suitable for in-situ use and real-time control;
- demonstration of agreement between theory and experiment for XRF measurement simple systems using the XRF sensor;
- demonstration of agreement between inductively coupled plasma (ICP) and XRF results over a wide variety of CIGS samples;
- initial design of hardware protecting XRF sensor in heated, Se ambient;
- resolution of a number of installation issues, including specification of measurement time versus sensor-to-sample distance, utilities requirements, and vibration restrictions;
- development of software for sensor operation and the automatic extraction of composition data; and interaction with National CIS R&D Team industrial partners to specify and adapt sensor functions.

14. SUBJECT TERMS
photovoltaics ; CuIn(Ga)Se_2 ; CIGS ; X-ray fluorescence ; optical emission spectroscopy ; in-situ sensors ; Thin film PV Partnership

15. NUMBER OF PAGES

16. PRICE CODE

17. SECURITY CLASSIFICATION OF REPORT	18. SECURITY CLASSIFICATION OF THIS PAGE	19. SECURITY CLASSIFICATION OF ABSTRACT	20. LIMITATION OF ABSTRACT
Unclassified	Unclassified	Unclassified	UL